JOURNAL OF CATALYSIS 125, 456–466 (1990)

CO-Induced Structural Changes of Rh on TiO_2 Support

D. A. BUCHANAN, M. E. HERNANDEZ,[1] F. SOLYMOSI,[2] AND J. M. WHITE

Department of Chemistry, University of Texas, Austin, Texas 78712

Received March 2, 1990; revised April 25, 1990

The behavior of Rh supported on TiO_2 has been studied as a function of oxidation and reduction temperature. Infrared spectroscopy of adsorbed CO and OH and X-ray photoelectron spectroscopy of Rh demonstrate the strong dependence of chemisorbed CO on the oxidation state of Rh and the importance of OH on TiO_2 in controlling the Rh dispersion process. Carbon monoxide exposure induces oxidative disruption of metallic Rh clusters at temperatures as low as 160 K. At temperatures above 473 K, CO exposure leads to reduction of oxidized Rh. © 1990 Academic Press, Inc.

INTRODUCTION

In studies of the hydrogenation of CO_2 and CO over Rh, titania was found to be the most effective support; the specific activities of the hydrogenations were almost two orders of magnitude higher than those on the less active Rh/SiO_2 (*1–5*). To achieve a high catalytic activity it was necessary to reduce the Rh/TiO_2 samples at 473–673 K; reduction at higher temperatures, which resulted in a decrease in the number of surface Rh atoms available for the reaction, was detrimental to the methanation of carbon oxides. Such Rh/TiO_2 catalysts were also active in the synthesis of oxygenated compounds (*5, 6*) and oxidized metal, Rh^+, has been proposed as the active center in their production (*7, 8*).

To elucidate the reaction mechanism, it is necessary to learn more about the nature of the interaction between carbon oxides and dispersed Rh. It is generally agreed that there are three primary carbonyl species, as originally determined by Yang and Garland (*9*) using IR spectroscopy: gem dicarbonyl, $Rh(CO)_2$, with asymmetric and symmetric bands at 2095 and 2027 cm^{-1}; linear, Rh_x–CO, at 2045–2062 cm^{-1}; and bridged, Rh_2–CO, at 1905–1925 or 1850 cm^{-1}. While the adsorption of CO on supported Rh has been the subject of numerous subsequent studies, a new and deeper insight into the nature of the CO–Rh interaction was obtained recently. Prins and co-workers (*10–12*), using EXAFS, demonstrated that the reduced Rh/Al_2O_3 contained small Rh crystallites (Rh_x) which were disrupted as a result of CO adsorption (298 K) and were postulated to be oxidized to Rh^+. Solymosi and Pasztor (*13–16*) followed this process by infrared spectroscopy and found that CO adsorption caused the disruption of both small and large crystallites. The presence of water vapor promoted disruption of Rh while hydrogen inhibited it. They also observed that at higher temperatures the effect of CO is reversed and leads to the reductive agglomeration of Rh^+. This was confirmed in a number of subsequent studies (*17–23*). Yates and co-workers (*17, 18*) found a direct correlation between the development of gem dicarbonyl, $Rh^+(CO)_2$, and the consumption of isolated OH groups on alumina. The effects of supports and additives on these processes were also examined (*16, 19, 24, 25*). On titania, no detailed studies concerning how the support influences the structure of rhodium have been performed so far.

The primary aim of the present work is to

[1] Summer Student. Present address: Department of Chemistry, University of Texas, El Paso, Texas.

[2] Permanent address: Reaction Kinetics Research Group, University of Szeged, Szeged, Hungary.

0021-9517/90 $3.00

establish the main characteristics of morphological changes of Rh, supported on titania, with particular attention given to the effects of reduction temperature and of OH groups on titania.

EXPERIMENTAL

Materials

Rh/TiO_2 (2 wt% Rh) was prepared by impregnating TiO_2 (Degussa P 25, BET area 50 m^2/g) with an aqueous solution of $RhCl_3 \cdot XH_2O$. After impregnation, the sample was dried in air at 383 K. In some cases, titania was calcined at 873 K in air for 6 h before impregnation. To prepare a sample for transmission infrared, the dried and pulverized Rh/TiO_2 was pressed into a tantalum mesh which had been spot-welded to two tantalum wires. Samples were resistively heated by passing current through the wires. A chromel–alumel thermocouple was spot-welded to the frame of the mesh. Further treatment was applied *in situ;* it consisted of oxidation at 573 K (100 Torr of O_2 for 60 min), evacuation at 573 K for 30 min, reduction at the selected temperature, between 473 and 673 K (100 Torr of H_2 for 60 min), and evacuation at the temperature of reduction for 30 min. All of the reagent gases mentioned above were used as received from the manufacturer (Union Carbide Corp.) without further purification.

For X-ray photoelectron spectroscopy (XPS), the sample (approx 25–40 mg) was pressed into a tantalum mesh which had been spot-welded to a thin foil of tantalum metal (1.2 × 1.8 cm) secured to the base plate of a heatable sampling rod (see below). A chromel–alumel thermocouple was placed in direct contact with the powder–mesh interface for temperature measurement.

Methods

Most of the infrared spectra were recorded with a Mattson Cygnus 100 FTIR system. The resolution was 4 cm^{-1} and 100 scans were averaged per spectrum. IR spectra were taken at the temperature of CO adsorption (~300 K) unless otherwise noted. Experiments were performed in a stainless-steel system, capable of ultrahigh vacuum, which was partitioned by a gate valve into two chambers. The system is described in detail in another paper (*26*). The preparation chamber has two CaF_2 windows (Harshaw) positioned to transmit the FTIR beam through the chamber to a mercury cadmium telluride (MCT) detector. External optics were continuously purged with dry nitrogen. Dosing pressures in the chamber were monitored by either a MKS baratron capacitance manometer or a Varian vacuum ionization gauge. The base pressure of the vacuum system was 1×10^{-8} Torr. Low-temperature IR measurements ($T <$ 300 K) were performed in a cell similar to that described by Knozinger and co-workers (*19, 25*). These spectra were recorded by a Specord M80 (Zeiss) spectrophotometer equipped with a data handling system.

TABLE 1

Adsorption of H_2 on 2 wt% Rh/TiO_2 at 300 K

Reduction temperature (K)	H/Rh
473	0.63
573	0.52
673	0.43

The dispersion of the rhodium was determined via H_2 adsorption at 298 K in a static system. Characteristic data are shown in Table 1.

XPS spectra were obtained on a Leybold–Heraeus LHS-12 surface analysis system equipped with a dual X-ray anode (Mg and Al) and an EA-11 hemispherical analyzer. The base operating pressure was 3.5×10^{-9} Torr. The data shown for this paper were obtained with Mg$K\alpha$ radiation (1253.6 eV) at 200 W (10K eV, 20 mA), operating at 40 eV pass energy. The FWHM of the Ag $3d_{5/2}$ peak was 0.91 eV. Peak posi-

tions were reproducible within 0.1 eV. Binding energy values were referenced to C (1*s*), defined as 284.6 eV. The sample treatment procedures were performed in a high-pressure chamber that is directly attached via a load-lock system to the XPS analysis chamber. A heatable sample rod moved the sample between the chambers.

RESULTS

Oxidative Disruption of Rh Crystallites

In our first experimental series the Rh/TiO_2 was reduced at 573 K and then CO was adsorbed at 300 K. Figure 1 shows representative spectra, and Fig. 2 shows the plot of the peak heights of two important rhodium carbonyl bands as a function of time and CO pressure. The adsoprtion pressure started at 1×10^{-6} Torr and was gradually raised. Spectral changes were followed in time at each CO pressure. At low pressure, Fig. 1A, a weak band appeared at 2030 cm^{-1} and is very likely due to CO linearly bonded to a metallic Rh_x cluster. The intensity of this band slowly increased with adsorption time. After 30 min another weak band developed at 2100 cm^{-1} and the band at 2030 cm^{-1} broadened. These spectral changes indicate the formation of gem dicarbonyl, $Rh^+(CO)_2$; the 2100 cm^{-1} band is its asymmetric stretch (*13–19, 21–25*). The symmetric stretch at 2030 cm^{-1} cannot be resolved at this pressure due to overlap of the Rh_x–CO band. In addition, we detected a weak, broad band at 1920 cm^{-1}, which is associated with bridge-bonded CO, Rh_2–CO. Another bridge-bonded CO at 1870 cm^{-1} can be distinguished at a CO pressure of 5×10^{-5} Torr.

The intensities of all these absorption bands increased with the CO pressure and adsorption time, and total saturation was not reached even at high (50 Torr) CO pressure. With increased exposure, the position of the Rh_x–CO band gradually shifted to higher frequencies; the maximum was 2075 cm^{-1}. As a result, the symmetric stretch of the gem dicarbonyl (2030 cm^{-1}) was detectable. When 50 Torr of CO was applied, the intensity of 2100 cm^{-1} band exceeded that of 2050–2070 cm^{-1} band, but the complete elimination of the latter band was not achieved even after the sample was kept in 50 Torr of CO for 50 h (Fig. 2E).

In another set of experiments, the effect

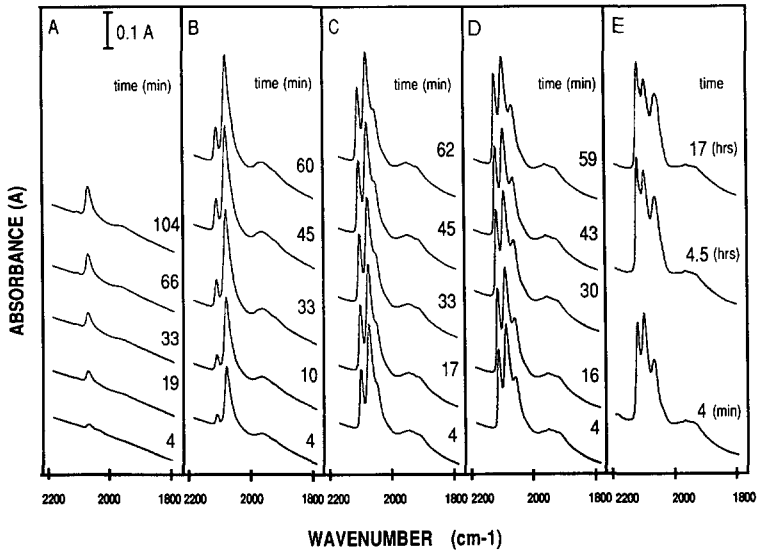

FIG. 1. Infrared spectra of adsorbed CO (dosed at 300 K) on 2 wt% Rh/TiO_2 reduced at 573 K. Pressures of CO were (A) 1×10^{-6}, (B) 5×10^{-5}, (C) 8×10^{-3}, (D) 5×10^{-1}, and (E) 50 Torr.

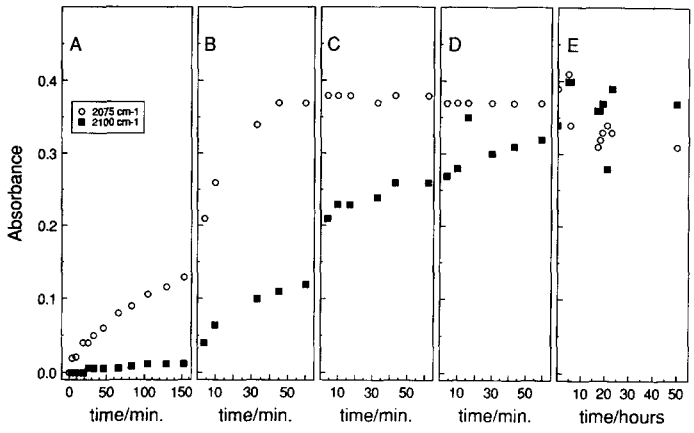

FIG. 2. Intensity changes of rhodium carbonyl bands from Fig. 1 as a function time and CO pressure at 300 K.

of sample reduction temperature was examined. These experiments were performed with one sample, which was regenerated by an oxidation–reduction treatment. The reduction temperature was varied between 473 and 673 K. The sample was exposed to a selected CO pressure for 10 min, then raised to the next CO pressure for another 10 min per each reduction temperature chosen. Spectra are shown in Figs. 3A–3C. Although the dominant spectral feature on Rh/TiO_2 (T_R = 473 K; T_R, reduction temperature) at low CO pressures was the linearly bonded CO, Rh_x–CO, the development of the twin band due to gem dicarbonyl occurred relatively easily. This process proceeded more slowly for samples reduced at higher temperatures.

In subsequent measurements the effect of adsorption temperature (90–285 K) on CO-induced surface processes was determined. A background spectrum of the clean Rh/TiO_2 powder was obtained at 90 K before exposure to CO(g) as shown by the bottom

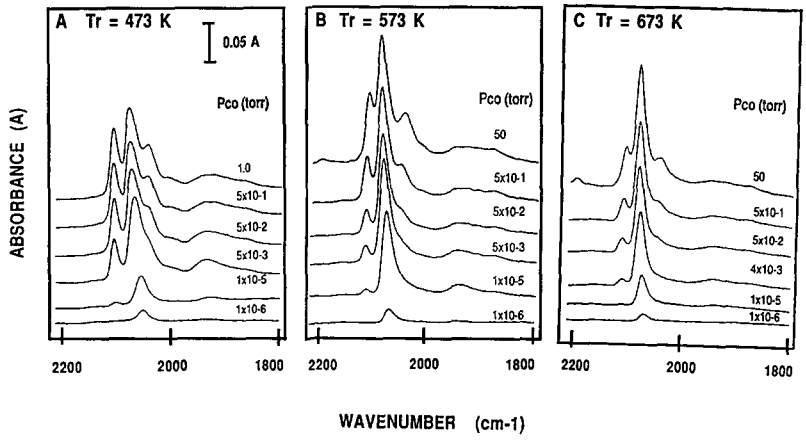

FIG. 3. Effects of reduction temperature on spectral changes observed for 2 wt% Rh/TiO_2 as a function of CO pressure at 300 K taken at 10-min intervals. (A) T_R = 473 K, (B) T_R = 573 K, and (C) T_R = 673 K.

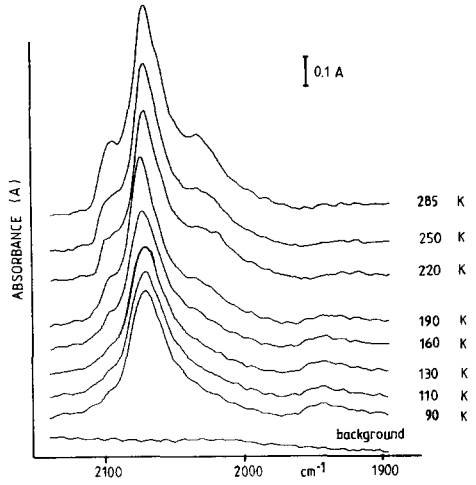

FIG. 4. Spectral changes observed during adsorption of 10 Torr of CO on 2 wt% Rh/TiO_2 (T_R = 573 K) at 90 K and gradual warming of the sample to higher temperatures.

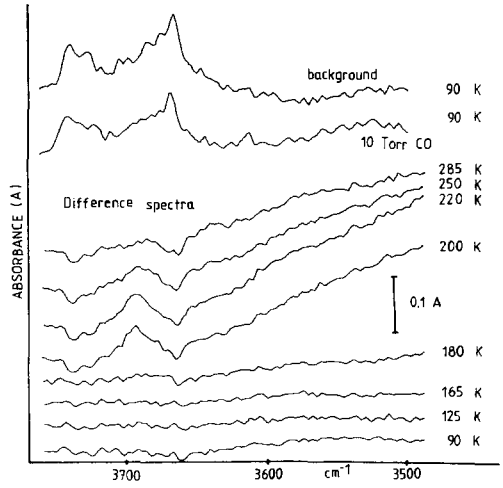

FIG. 5. Spectral changes in the OH frequency range of 2 wt% Rh/TiO_2 (T_R = 573 K) during CO adsorption at 90 K and subsequent higher temperatures. Except for the upper two spectral traces, different spectra are shown.

spectral trace of Fig. 4. After exposure to 10 Torr of CO at 90 K, the sample (T_R = 573 K) was heated gradually to higher temperatures. Thus at 90 K, there were two intense bands at 2155 and 2180 cm^{-1} (not shown in Fig. 4). These were eliminated by heating to 170–180 K. The band at 2155 cm^{-1} is attributed to H-bonded CO. The band at 2180 cm^{-1} can be assigned either to CO coordinated to impurity Al^{3+} sites in the titania (*19*) or to CO weakly chemisorbed on the titania support itself (*20*). However, Fig. 4 does show that more stable bands appeared at 2070 and 1920 cm^{-1} with increasing temperature. Weak bands due to gem dicarbonyl (2095 and 2033 cm^{-1}) were detected first at 160 K; their intensities increased with temperature. An increase was also noted in the intensity of the linearly bonded CO band at 2070 cm^{-1}.

Several attempts were made to follow spectral changes in the O–H stretching frequency range, parallel to the development of $Rh^+(CO)_2$ species. This was done in the course of warming the sample from 90 K (Fig. 5) and also while increasing the CO pressure at 300 K (Fig. 6). The top trace of Fig. 5 shows the clean spectrum at 90 K (T_R = 573 K) which exhibited bands at 3735 and 3663 cm^{-1} before CO adsorption. Just below this trace is the result of adsorption of 10 Torr of CO at 90 K. Then, beginning at the bottom of Fig. 5, the difference spec-

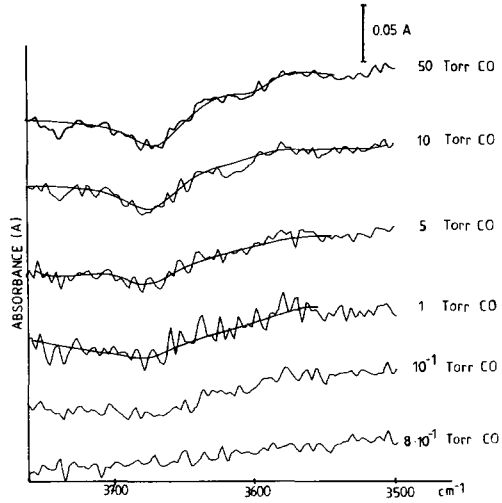

FIG. 6. Difference spectra collected in the OH frequency range of 2 wt% Rh/TiO_2 (T_R = 573 K) as a function of CO pressure at 10 min intervals.

tra are shown (i.e., CO adsorption spectra minus the clean spectrum) as a function of increasing temperature. Negative bands at 3735 and 3663 cm^{-1} appeared first at 190–200 K, when the development of bands due to gem dicarbonyl (2095 and 2033 cm^{-1}) were also detected (see Fig. 4). In some experiments a band at 3427 cm^{-1} whose intensity was rather weak and whose position varied ±20 cm^{-1} was also seen.

The changes occurring in the OH stretching frequency as a function of increasing CO pressure in Fig. 6 are seen more clearly with difference spectra. While not shown, a clean spectrum of Rh/TiO_2 was taken at 300 K just prior to CO adsorption. All subsequent spectra were recorded by subtracting out this clean spectrum. Thus when the CO pressure was increased, a negative band was found to develop at 3670 cm^{-1} once the CO pressure reached 1 Torr, indicating loss of the hydroxyl (OH) moiety. The curve fits outlining the spectra were added to guide the eye; they are not a model fit.

The results of Fig. 7 (shown as transmission spectra) demonstrate the influence of water coadsorption. The background spectrum of Rh/TiO_2 was recorded at 300 K prior to gas adsorption. Then a spectrum was recorded upon adsorption of 10 Torr of CO at 300 K for 10 min (Fig. 7A). A similar

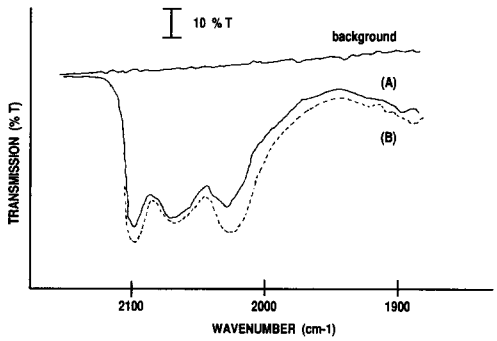

FIG. 7. Spectra (transmission) observed following adsorption on 2 wt% Rh/TiO_2 (T_R = 673 K) for 10 min at 300 K (A) in the presence of 10 Torr of CO, and (B) in the presence of a mixture of 10 Torr of CO and 2 Torr of H_2O.

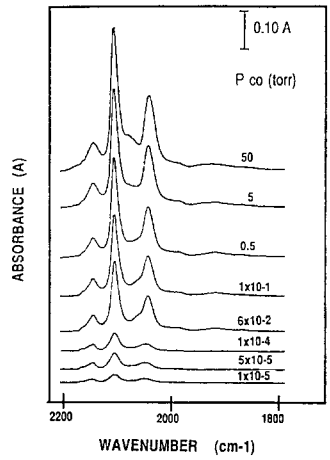

FIG. 8. Effect of CO pressure at 300 K on infrared spectra taken at 10-min intervals for a thermally treated (vacuum, 2 h, 573 K) unreduced 2 wt% Rh/TiO_2.

experiment was performed with a new sample which was exposed to a mixture of 10 Torr of CO and 2 Torr of H_2O at 300 K for 10 min (Fig. 7B). In this latter case, the gem dicarbonyl bands (2100 and 2030 cm^{-1}) are slightly more intense. This result agrees with that found for CO adsorption on Rh/Al_2O_3 (*13*).

In order to explain the time-dependent development of $Rh^+(CO)_2$ species (Figs. 1–3), it is important to know the nature of CO adsorption on Rh^+ sites. To that end, spectral changes of unreduced Rh/TiO_2 were followed in the presence of CO at 300 K. The sample was preheated in vacuum at 573 K for 2 h and not subjected to hydrogen reduction treatment. Some selected spectra taken at 10 min intervals are depicted in Fig. 8. Four species were observed in the CO spectral region: intense bands at 2109 and 2040 cm^{-1} due to $Rh^+(CO)_2$; a less intense band at 2147 cm^{-1}, which could be attributed to Rh^{3+}–CO species (*24*); and very weak bands at 2080 and 1930 cm^{-1}, which are associated with Rh_x–CO and Rh_2–CO, respectively.

XPS Measurements

To obtain an independent estimate of the state of Rh, we measured XPS spectra be-

fore and after the reduction in H_2 and then after exposure to CO. The spectra in Figs. 9A–9D show definite changes in the binding energy values of the rhodium 3*d* features as a function of H_2 treatment and CO adsorption experiments. These changes can be interpreted in terms of changes in oxidation state. After H_2 reduction at 573 K, the oxidized rhodium salt (assumed Rh^{3+} and Rh^{+}) is reduced to metallic-like rhodium (see Table 2) evidenced by the 6.2-eV downshift in binding energy as seen in Figs. 9A and 9B. Subsequent carbon monoxide adsorption at 300 K reversed this process to give a sample with comparably more oxidized rhodium species. Interestingly, carbon monoxide adsorption at an elevated temperature (523 K) appeared to shift, albeit slightly, the primary Rh $3d_{5/2}$ peak at 312.0 eV to 311.4 eV (Figs. 9C and 9D), suggesting a partial rereduction of the rhodium species. These results are consistent with the IR experiments (Figs. 3B, 10B–10D) which showed gem dicarbonyl as well as linear and bridged carbonyl species that are associated with rhodium in the +1 and 0 oxidation states, respectively.

TABLE 2

Binding Energy Values for Major XPS Peaks (Mg$K\alpha$ Rays) Adjusted for Surface Charging

	Rh $3d_{5/2}$	C 1*s*
(A) Clean	312.8	287.1, 284.6[a]
(B) After H_2(573K)	306.6	284.6[a] (Weak)
(C) After CO(300K)	312.0	284.6[a] (Weak)
(D) After CO(523K)	311.4	284.6[a] (Weak)
Rh (111)	307.1[b]	
Rh foil	307.0[c]	
Rh foil	307.3[d]	

[a] Assigned as residual carbon
[b] *Surf. Sci.* **147,** 252 (1984).
[c] *J. Amer. Chem. Soc.* **107,** 3139 (1985).
[d] *J. Catal.* **80,** 472 (1983).

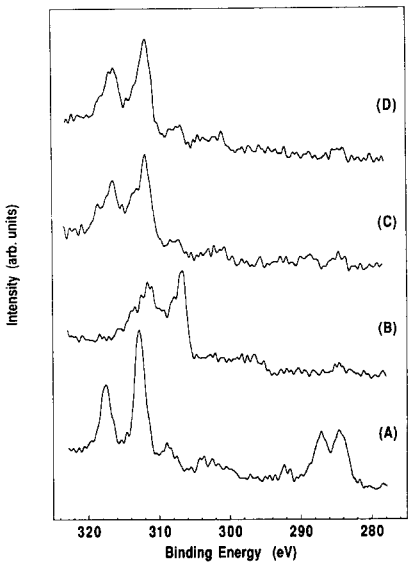

FIG. 9. Rh(3*d*) and C(1*s*) XPS spectra of (A) 2 wt% Rh/TiO_2 sample, evacuated for 120 min; (B) after H_2 reduction treatment (573 K, 100 Torr, 60 min); (C) after CO adsorption (300 K, 50 Torr, 60 min); and (D) after second CO adsorption (523 K, 50 Torr, 120 min).

Reduction by CO

Having examined the dispersing and accompanying oxidation effects of CO at $T \leq$ 300 K, we turn to CO adsorption at higher temperatures, where its reducing properties come into prominence. In order to study this process more closely, an attempt was made to convert Rh_x–CO and Rh_2–CO into $Rh^{+}(CO)_2$ species by treating the sample (T_R = 573 K) with CO at elevated temperatures (>300 K). Heating to 448 and 473 K in the presence of 50 Torr of CO caused spectral changes after 5 h (Fig. 10A) which could be compared to data collected at 300 K (Fig. 3B). At 523 K, however, the intensity of the gem dicarbonyl bands gradually decreased after several hours without producing new bands of significant intensity (Figs. 10B–10F). A weak band can be distinguished at 2050–2063 cm^{-1}, which remained after complete elimination of the twin band (Fig. 10F).

Upon cooling the sample to room temper-

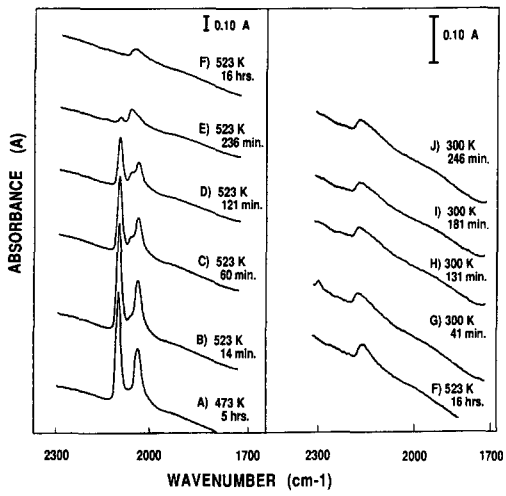

FIG. 10. Changes in infrared spectrum of adsorbed CO on 2 wt% Rh/TiO_2 (T_R = 573 K) in the presence of 50 Torr of CO. Before the sample was warmed to selected temperatures, it was treated with 50 Torr of CO at 300 K for 3 h. Then it was heated (A–F) and recooled (G–J) while maintaining 50 Torr pressure.

ature in the presence of 50 Torr of CO (Figs. 10G–10J), the intensity of the singular band at 2050 cm^{-1} remained constant and there was no indication of gem dicarbonyl band reformation even after several hours.

DISCUSSION

Oxidative Disruption

The results presented unambiguously show that the adsorption of CO on reduced Rh/TiO_2 induced a morphological change of supported Rh. The nature of the structural change depends on the temperature of CO adsorption. We discuss first the data obtained at 300 K or below.

The reduction of Rh/TiO_2 is complete at 573 K (*28*) and the adsorption of CO on Rh_x crystallites occurs readily at 300 K. Thus, the enhancement of the absorption band for only the linearly bonded CO, Rh_x–CO, at low pressure (Figs. 1A and 1B) suggests that CO adsorption causes disruption of larger Rh_x crystallites into smaller ones.

$$Rh_x + CO = Rh_x\text{–}CO \qquad (1)$$

$$Rh_x\text{–}CO + CO = Rh_{x-y}\text{–}CO + Rh_y\text{–}CO \qquad (2)$$

As a result, the concentration of linearly bonded CO is increased. After longer contact time with CO, the absorption bands of $Rh^+(CO)_2$ at 2100 and 2030 cm^{-1} gradually developed. This indicates that in the disruption process a more reactive, perhaps isolated, Rh^0 atom is formed,

$$Rh_y\text{–}CO + CO = Rh_{y-1}\text{–}CO + Rh^0\text{–}CO, \qquad (3)$$

where Rh^0 is an isolated Rh atom, and the oxidation of Rh^0–CO to Rh^+ proceeds easily. The occurrence of this process can be detected even at the lowest CO pressure (1×10^{-6}–5×10^{-5} Torr).

In the explanation of the time dependence of the development of gem dicarbonyl, we can exclude the possibility that the reduced sample contains unreduced Rh^+ centers and that the adsorption of CO would be a slow process on Rh^+ sites. This could perhaps be the case for a sample reduced at 473 K, but not for Rh/TiO_2 reduced at 673 K, which showed similar behavior (Figs. 3A and 3C). In addition, the adsorption of CO on thermally treated but unreduced Rh/TiO_2 (which contained Rh^{3+} and Rh^+) quickly produced intense bands at 2109 and 2040 cm^{-1} (Fig. 8) and there were no strong time-dependent spectral changes. This suggests a fast uptake of CO by Rh^+ sites. Accepting the view that the adsorption of CO is a fast process on both the Rh_x crystallite and on the Rh^+ site, the relative increase in the intensity of $Rh^+(CO)_2$ to Rh_x–CO bands (Figs. 1 and 2) also supports the transformation of Rh_x into Rh^+ during CO adsorption.

The observation that with increasing reduction temperature, the transformation of Rh_x to Rh^+ proceeds more slowly is in accord with the expectation that high temperature reduction produces larger Rh crystallites, the disruption of which by CO adsorption is more difficult (*13*). The extended reduction of titania at and above 773 K and the decoration of Rh by titania at this

temperature (*29*) prevented us from performing more detailed measurements with the high-temperature-reduced samples.

With regard to the oxidation of isolated Rh^0 atoms, two possibilities can be considered: (i) the dissociation on Rh^0 of CO, to form adsorbed carbon and oxygen atoms, and the subsequent oxidation of Rh^0 by chemisorbed oxygen,

$$Rh^0 + O_{(a)} = Rh^+ + O^-_{(a)} \qquad (4)$$

and (ii) oxidation of Rh^0 by the OH groups of the support

$$Rh^0 + OH^- = Rh^+ + O^{2-}_{(a)} + \tfrac{1}{2}H_2. \qquad (5)$$

Although in the case of Rh/Al_2O_3 the former process was advocated by a number of authors (*11, 12, 24, 30*), it was completely discarded by Solymosi and Pasztor (*13, 14*), as the dissociation of CO on Rh/Al_2O_3 occurs only above 523 K (*31, 32*). It is true that Rh/TiO_2 is much more active in this process than Rh/Al_2O_3; the lowest temperature determined for the dissociation of CO was about 473 K (*32, 33*). We may speculate that the CO dissociates on Rh/TiO_2 at even lower temperatures, e.g., at 300–373 K, but its detection requires a more sensitive technique. However, the formation of gem dicarbonyl occurred far below room temperature, 160–170 K (Fig. 4), where the dissociation of CO can certainly be excluded. These results strongly suggest that the oxidation of Rh^0 occurs by the process involving OH groups of the titania (Eq. (5)).

Two findings support this conclusion: (i) the formation of gem dicarbonyl proceeds more readily with injection of water into CO gas (Fig. 7), and (ii) the attentuation of adsorption bands of OH groups from titania (Figs. 3B and 4) parallels the development of bands due to $Rh^+(CO)_2$ species (Figs. 6 and 5).

The second observation deserves more detailed consideration. The chemistry of OH groups on titania has been the subject of a number of IR spectroscopic studies (*20, 34–38*). Several absorption bands have been detected in the frequency range of 3400–3750 cm^{-1}; their existence and intensity depended sensitively on the pretreatment temperature, e.g., on the degree of dehydroxylation. On our sample, we observed bands at 3735 and 3663 cm^{-1} which can be assigned to isolated OH groups (*34, 36*). Spectral changes presented in Figs. 5 and 6 indicate that the OH groups responsible for these bands are consumed when $Rh^+(CO)_2$ species are formed. The involvement of OH groups in the oxidative disruption of Rh_x crystallites is not as clear as in the case of Rh/Al_2O_3, where a linear correlation was found between the decay in the sum of absorbance of OH bands at 3735 and 3679 cm^{-1} and the increasing intensity of $Rh^+(CO)_2$ bands (*17, 18*). One possible reason is that the oxidative disruption process of Rh_x crystallite on titania occurs more slowly than on alumina and/or the partial regeneration of isolated OH groups may proceed from other OH species during the time-dependent oxidative disruption process. Alternatively, other OH groups on titania (not detected by our measurements) can also participate in the reaction.

The partial oxidation of Rh_x clusters during CO adsorption at 300 K has been confirmed by XPS measurements. We obtained clear evidence for a strong Rh(3*d*) binding energy increase (Table 2).

Evidence of Reduction by CO

When the sample was heated to 523 K in the presence of CO, the intensity of bands due to gem dicarbonyl gradually decreased with little indication for the enhancement of Rh_x–CO species (Fig. 8). This would suggest that at this temperature the CO desorbs from Rh^+ sites,

$$Rh^+(CO)_2 = Rh^+ + 2CO, \qquad (6)$$

but does not induce the reductive agglomeration of Rh^+; i.e.,

$$2Rh^+(CO)_2 + O^{2-} = Rh^0\text{–}CO + CO_2 + 2CO \qquad (7)$$

$$xRh^0 = Rh_x\text{–}CO. \qquad (8)$$

This behavior contrasts with that of the CO–Rh/Al_2O_3 system (*13, 18, 21*), where reductive agglomeration to Rh_x clusters did occur. If CO desorbs at 523 K with no change in Rh, then one expects that cooling to room temperature in the presence of CO should produce bands of gem dicarbonyl with the same intensities as observed before heating. However, after adding CO up to 16 h, we did not obtain bands corresponding to the $Rh^+(CO)_2$ species and even the weak band at 2070 cm^{-1} due to Rh_x–CO intensified only slightly. This finding suggests that desorption of CO is, at 523 K, accompanied by structural changes, which lead to inactive Rh crystallites. The fact that exposure to CO at 300 K did not yield gem dicarbonyl even after several hours indicates that these structural changes are difficult to reverse. They may involve a reaction between Rh and titania.

Finally, we compare the influence of different supports on the CO-induced structural changes of Rh. Although the rate of oxidative disruption certainly depends on the size of Rh crystallites (*13, 18, 19*), we can safely conclude that this process occurs more slowly on titania than, for instance, on alumina. Adsorption of CO on Rh/Al_2O_3 (T_R = 473–573 K) produced in most cases only a gem dicarbonyl at 300 K without evidence for linearly bonded CO (*13, 14, 17–19, 21*). In the case of Rh/TiO_2, the Rh_x–CO band was a prominent spectral feature even after several hours (Fig. 1). This difference cannot be due to different crystallite sizes as the dispersion of Rh reduced at 473 and 573 K (Table 1) is practically the same as that obtained for Rh/Al_2O_3 reduced at the same temperature (*13*). This suggests that the decisive step on both samples is that oxidation of isolated Rh atoms by OH groups. We believe that the OH groups on alumina are more efficient oxidizing agents than those on titania.

CONCLUSIONS

1. Adsorption of CO on Rh/TiO_2 induces an oxidative disruption of Rh_x crystallites and leads to gem dicarbonyl, $Rh^+(CO)_2$ species.

2. The above reaction occurs for temperatures as low as 160–180 K, where the dissociation of CO on Rh/TiO_2 is excluded.

3. The fact that the presence of water vapor enhances this process and OH groups on titania are consumed during the formation of $Rh^+(CO)_2$ species suggests the involvement of isolated OH groups of titania in the oxidation of Rh_x clusters.

4. Above 473 K, the adsorption of CO leads to partial reduction of Rh^+ to Rh^0 but not to the reformation of Rh_x crystallites.

ACKNOWLEDGMENTS

This work was supported in part by the US Department of Energy, Office of Basic Energy Sciences. One of us (F. Solymosi) acknowledges partial support by the Fulbright Foundation. We thank Kristi Allan and Professor Alan Campion for their generous assistance with XPS measurements.

REFERENCES

1. Solymosi, F., Erdohelyi, A., and Bansagi, T., *J. Catal.* **68,** 371 (1981).
2. Solymosi, F., Tombacz, I., and Kocsis, M., *J. Catal.* **75,** 78 (1982).
3. Solymosi, F., Tombacz, I., and J. Koszta, *J. Catal.* **95,** 578 (1985).
4. Vannice, M. A., *J. Catal.* **74,** 199 (1982).
5. Katzer, J. R., Sleight, A. W., Gajardo, P., Michel, J. B., Gleason, E., and McMillan, S., *Faraday Discuss. Chem. Soc.* **72,** 121 (1982).
6. Takeuchi, A., and Katzer, J. R., *J. Catal.* **82,** 351 (1983).
7. Driessen, J. M., Poels, E. K., Hindermann, J. P., and Ponec, V., *J. Catal.* **82,** 26 (1983).
8. Watson, P. R., and Somorjai, A. G., *J. Catal.* **72,** 347 (1981).
9. Yang, A. G., and Garland, C. W., *J. Phys. Chem.* **61,** 1504 (1957).
10. Van't Blik, H. F. J., Van Zon, J. B. A. D., Huizinga, T., Vis, J. C., Koningsberger, D. C., Prins, R., *J. Phys. Chem.* **87,** 2264 (1983).
11. Van't Blik, H. F. J., van Zon, J. B. A. D., Huizinga, T., Vis, J. C., Koningsberger, D. C., and Prins, R., *J. Amer. Chem. Soc.* **107,** 3139 (1985).
12. Van't Blik, H. F. J., van Zon, J. B. A. D., Koningsberger, D. C., and Prins, R., *J. Mol. Catal.* **25,** 379 (1984).
13. Solymosi, F., and Pasztor, M., *J. Phys. Chem.* **89,** 4783 (1985).
14. Solymosi, F., and Pasztor, M., *J. Phys. Chem.* **90,** 5312 (1986).

15. Solymosi, F., and Pasztor, M., *J. Catal.* **104,** 312 (1987).
16. Solymosi, F., Pasztor, M., and Rakhely, G. J., *J. Catal.* **110,** 413 (1988)
17. Basu, P., Panayotov, D., and Yates, J. T., Jr., *J. Phys. Chem.* **91,** 3133 (1987).
18. Basu, P., Panayotov, D., and Yates, J. T., Jr., *J. Amer. Chem. Soc.* **110,** 2074 (1988).
19. Zaki, M. I., Kunzmann, G., Gates, B. C., and Knozinger, H., *J. Phys. Chem.* **91,** 1486 (1987).
20. Yates, D. J. C., *J. Phys. Chem.* **65,** 746 (1961).
21. Solymosi, F., and Knozinger, H., *J. Chem. Soc. Faraday Trans. 1,* **86,** 389 (1990).
22. Dictor, R., and Roberts, S., *J. Phys. Chem.* **93,** 2526 (1989).
23. Solymosi, F., Bansagi, T., and Novak, E., *J. Catal.* **112,** 183 (1988).
24. Bergeret, G., Gallezot, P., Gelin, P., Ben Taarit, Y., Fefebre, F., Naccache, C., and Shannon, R. D., *J. Catal.* **104,** 279 (1987).
25. Zaki, M. I., Tesche, B., Kraus, L., and Knozinger, H., *SIA, Surf. Interface Anal.* **12,** 239 (1988).
26. Cannon, K. C., Jo, S. K., and White, J. M., *J. Amer. Chem. Soc.* **111,** 5064 (1989).
27. Conesa, J. C., Sainz, M. T., Soria, J., Munuera, G., Rives-Arnau, V., and Munoz, A., *J. Mol. Catal.* **17,** 231 (1982).
28. Worley, S. D., Rice, C. A., Mattson, G. A., Curtis, C. W., Guin, J. A., and Tarrer, A. R., *J. Phys. Chem.* **86,** 2714 (1982).
29. Tauster, S. J., *in* "Metal-Support Interactions in Catalysis, Sintering, and Redispersion" (Scott A. Stevenson, J. A. Dumesic, R. T. K. Baker, and Eli Ruckenstein, Eds.), p. 128. Van Nostrand Reinhold, New York, 1987.
30. Primet, M., *J. Chem. Soc. Faraday Trans. 1* **74,** 2570 (1978).
31. Solymosi, F., and Erdohelyi, A., *Surf. Sci.* **110,** 1630 (1981).
32. Erdohelyi, A., and Solymosi, F., *J. Catal.* **84,** 446 (1983).
33. Orita, H., Naito, S., and Tamaru, K., *J. Catal.,* **112,** 176 (1988).
34. Primet, M., Pichat, P., and Mathieu, M.-V., *J. Phys. Chem.* **75,** 1216 (1971).
35. Jackson, P., and Parfitt, G. D., *Trans. Faraday Soc.* **67,** 2469 (1971).
36. Morishige, K., Kanno, F., Ogawara, S., and Sasaki, S., *J. Phys. Chem.* **89,** 4404 (1985).
37. Munoz, A., Gonzalez-Elipe, A. R., Munuera, G., Espios, J. P., and Rives-Arnau, V., *Spectrochim. Acta* **12,** 1599 (1987).
38. Mochida, I., Fujitsu, H., Ikeyama, N., *J. Chem. Soc. Faraday Trans. 1* **83,** 1427 (1987).
39. Solymosi, F., and Rasko, J., *J. Catal.* **115,** 107 (1989).